Academic Journal of Science and Technology
ISSN: 2771-3032 | Vol. 13, No. 3, 2024

Research on the Structural Design of a Nail-tooth Roller for Peanut Shelling

Rongrong Dai, Bo Zhao

Geely University of China, Chengdu 641402, China

Abstract: Peanut, as an important grain and oil crop, requires shelling before oil pressing, consumption, or planting. To address the issue of labor shortages resulting from population aging, this paper presents a peanut shelling mechanism using a nail-tooth roller method to tackle this problem. Based on the structure of peanuts, the characteristics of shelling are analyzed, and a structural design employing motor-driven and a combined cleaning method of "vibrating screen + air selection" is adopted. Finite element analysis is conducted on critical components to verify their structural compliance with stiffness and strength requirements, while also validating the feasibility of the peanut sheller.

Keywords: Peanuts; Shelling Machine; Vibration Screen; Fan.

1. Introduction

Peanuts are significant grain and oil crops, and they are also nutritionally rich as a food source due to their high protein content. A simple structural design for peanut shelling aims to address the issue of mechanized peanut shelling, while also tackling the labor shortage problem caused by population aging and achieving cost savings and efficiency enhancements. On one hand, it fulfills the material and cultural needs of the general public for peanuts as a consumer food product. On the other hand, it reduces production costs and enhances the market competitiveness of peanut-based products.

2. Design Principle of Peanut Shucking

As shown in Figure 1, the peanut shelling device consists of a series of key components, including belt transmission, ventilation equipment, power motor, screening vibrator, nail-shaped roller, grid-like screen, and guiding funnel. Among them, the nail-shaped roller and grid-like screen play the main roles in the operation. During the working process, the diameter of the peanut shells is larger than the grid gaps, so they cannot pass through and continue to be frictioned by the nail-shaped roller. Conversely, the peanut kernels, due to their smaller size than the grid intervals, fall through and land on the vibrating screen of the next layer. At the same time, the inclined spiral surface guides the peanut kernels and shells into the subsequent processing flow, accompanied by rotational and linear movements. This process continues until the peanut shells and kernels are completely separated and eventually flow into the discharge port. The ventilation equipment helps to clean impurities between the peanut shells and kernels, while the vibrating screen removes small, low-quality peanut kernels. The backbone of the entire device is the sturdy frame, which provides a stable foundation for the coordinated operation of all components.

In the architecture of the cleaning device, an independently driven fan occupies a central position. The electric motor installed below is responsible for driving the coordinated operation of the nail-tooth roller and vibrating screen. Once this process is initiated, the shelled peanuts first enter the device and are fed into the rubbing cylinder, undergoing gentle pressing and rolling. At the same time, the peanuts are guided forward by the spiral conveying system. The shelled peanuts and remaining shell debris then fall into the lower area, followed by the combined operation of the fan and vibrating screen, which performs a precise screening to completely separate the peanuts from the shell debris.

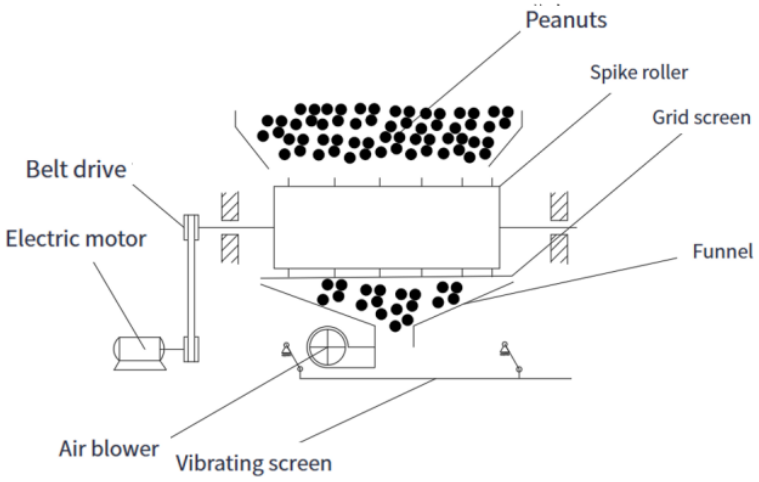

Figure 1. Structural diagram

3. Kneading Teeth Structure Design

The rubbing teeth are important and core working components for the rubbing process, and their performance and lifespan determine the working quality and stability of the entire machine. The rubbing teeth are installed on the main shaft, and the electric motor drives the shaft to rotate rapidly through belt transmission, causing the rubbing teeth to strike the peanuts. To facilitate the discharge of remaining peanut shells, the rubbing teeth are designed in a spiral shape, which aids in the expulsion of peanut shells from the rubbing teeth.

3.1. Analysis of the Layout of Rubbing Rollers

In the meticulous study of agricultural machinery, attention has been paid to the design elements of small rubbing machines. The number of rubbing teeth is crucial to the machine's performance, typically ranging between 7 and 11. In theory, more teeth can provide deeper rubbing, but this also implies higher energy consumption and cost investment. In seeking a balance between efficiency and economic benefits, the decision was made to use a smaller number of teeth, specifically a setting of 7 teeth. This choice not only considers the rubbing effect of the machine but also takes into account the operating costs.

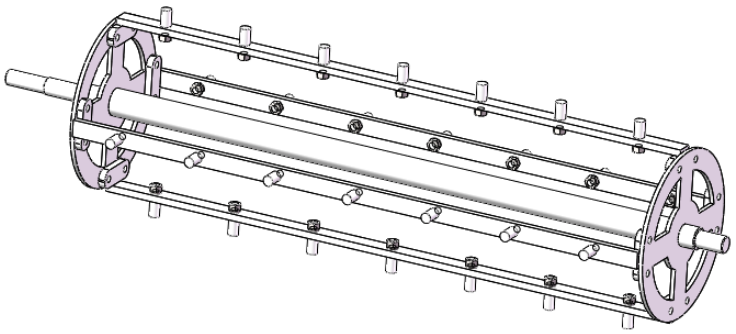

Figure 2. Rolling roller

In the illustration provided in Figure 2, the rubbing teeth are mounted on a tooth bar. Considering that the tooth bar is prone to wear and tear during operation, regular inspections and maintenance are necessary. Therefore, the innovative aspect of this design lies in the use of threaded connections to attach the tooth bar to circular plates at both ends. Compared to welding technology, this connection method facilitates a more convenient installation and replacement process.

3.2. Design and Verification of Installation Strip Structure

In the process of installing rubbing teeth, the key component is the tooth bar, which must possess adequate hardness. To accommodate various assembly methods, a Q235A steel plate with a thickness of 8mm is selected to ensure stability during the connection with the circular end plates. Its structure is illustrated in Figure 3 below:

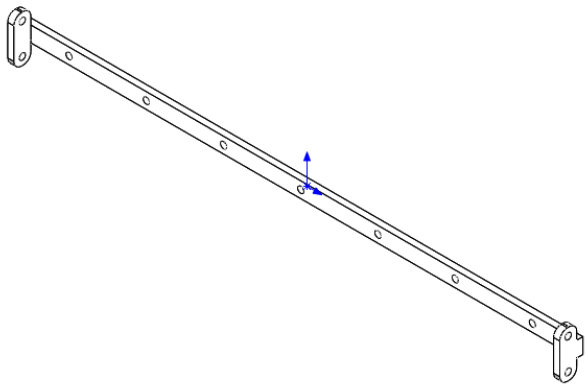

Figure 3. Rub the rack

To verify its feasibility, we conducted a stiffness calculation. Q235 steel can be directly processed and formed for this purpose. Due to the large loads and high operating speeds, all components are fixed using geometric shapes. During the load verification process, we considered a scenario where the load acts on the system in a direction perpendicular to the tooth surface. Each rubbing tooth can withstand a maximum force of 12 Newtons, so when seven rubbing teeth are combined, the total force they can withstand reaches 84 Newtons. For safety reasons, a safety factor of 1 was selected, meaning the applied test load is 84 Newtons. In the experiment, a configuration with fixed ends was chosen for this verification test. The results are shown in Figures 4 and 5.

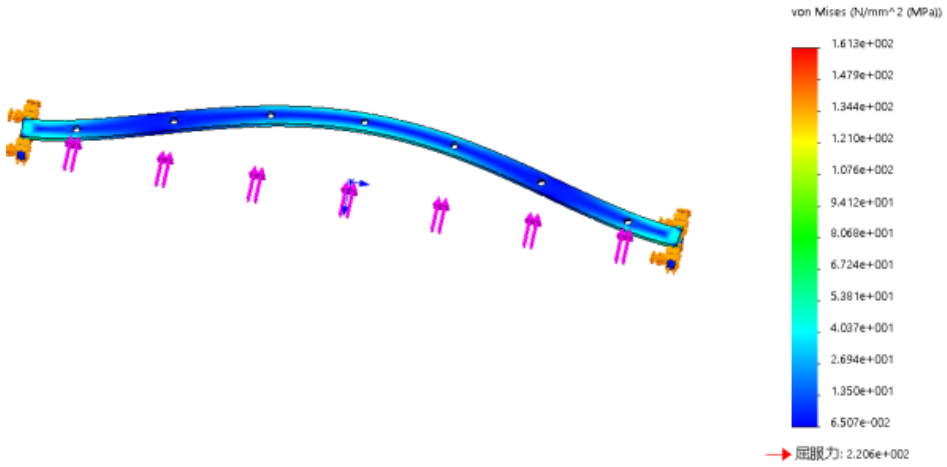

Figure 4. Stress distribution diagram

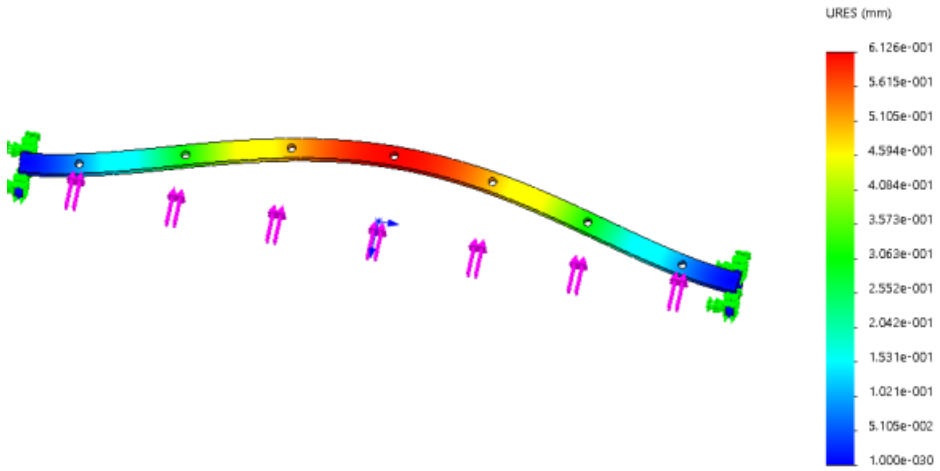

Figure 5. Displacement distribution

By observing Figures 2-3 and 2-4, the maximum stress value experienced by the driving shaft is 161.3 MPa, with a maximum displacement of 0.6 mm. In comparison, the yield strength of conventional carbon steel materials is 220.59 MPa. For safety reasons, a conservative safety factor of 1.2 is selected. Using this safety factor, more precise data can be obtained by applying the formula (1) for this application.

$$\sigma \leq [\sigma] \tag{1}$$

$$161.3Mpa < \frac{220.59}{1.2} = 183.83Mpa \tag{2}$$

As shown above, the strength and stiffness meet the strength requirements.

3.3. Structure design of kneading teeth

To achieve perfect rubbing of peanuts, the rubbing teeth, which are responsible for applying the striking and friction, play a crucial role, and the choice of their characteristics directly affects the performance of the entire device. When exploring material strategies, special attention was given to ensuring ease of operation and smooth rotation. Based on this, the following structural design was constructed, as shown in Figure 6:

Length L=20mm, diameter d=12mm;

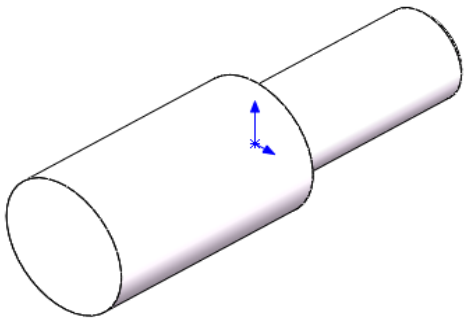

Figure 6. Gear kneading

3.4. Design of circular grid screen structure

To effectively separate peanut kernels and ensure smooth transportation, a special circular grid device has been designed. This device ensures that peanuts have sufficient time for thorough contact when passing through the rubbing tooth roller, thereby achieving the desired separation effect. The spacing size of the grid has been carefully calculated and set at approximately 10mm. Peanuts smaller than this size will naturally fall through and complete the separation process. Meanwhile, considering that the length of the peanuts needs to be similar to the tooth roller to ensure smooth transportation, relevant data has been referenced, which indicates that the diameters of most peanut cores are

concentrated between 10mm and 15mm. Based on these data, a grid structure with a gap size of about 10mm has been designed, as shown in Figure 7. To reduce potential damage to peanuts while they pass through, sturdy steel plates have been used for cutting, and 6mm round steel has been employed for connection. During installation, the grid is securely fixed to the side wall of the machine frame using bolts to ensure stability and reliability.

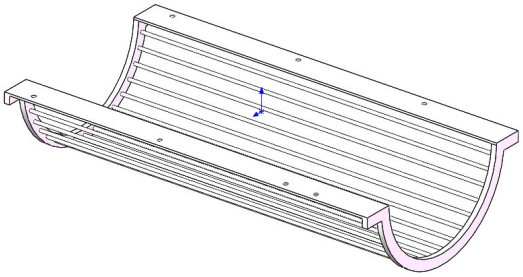

Figure 6. Concave plate composition

4. Cleaning Structure Design

Vibrating screens are widely used for the classification of materials. Their operating mechanism relies on the difference between the size of particles and the size of the sieve holes: particles smaller than the hole diameter will pass through and fall naturally, while those larger than the holes will remain on top. However, a potential issue arises when the equipment is stationary, as larger particles may sometimes link together to form a "bridge," hindering the falling process. To address this problem, vibrating elements are introduced to stimulate the material through rhythmic vibrations, facilitating smooth classification and screening. This vibration strategy not only breaks the potential "bridging" state but also enhances the efficiency of material sorting.

4.1. Vibrating screen type selection

There are mainly three types of vibrating screens, distinguished by their different motion trajectories: (1) Circular vibrating screen; (2) Linear vibrating screen; (3) High-frequency resonant screen.

The different motion characteristics of the three types of vibrating screens lead to distinct operating modes. Circular vibrating screens tend to adopt a multi-batch, intermittent operation mode. While this results in excellent material classification, their work schedule flexibility is limited by theoretical settings. In contrast, the screening process of linear vibrating screens is closely related to the length of the screening surface and the vibration frequency, with an increase in frequency reducing the screening duration. It is worth noting that linear vibrating screens excel in continuous operations due to their design that avoids internal conflicts and utilizes the principle of high-frequency vibration, particularly demonstrating high efficiency in the screening of fine particles. Therefore, based on these considerations, a linear vibrating screen appears to be more suitable for peanut screening applications. It can effectively remove impurities such as pebbles while accommodating the continuous operation requirements of peanut shellers.

4.2. Analysis of the motion of the vibrating screen mechanism

Under the scientific principles of vibration, the path of peanuts moving on the screen is deeply influenced by the two major factors of amplitude and frequency. Assuming that the angle formed between the screen surface and the horizontal plane is α, it is necessary to further explore the key angle that determines the vibration path, and the force analysis is shown in Figure 8.

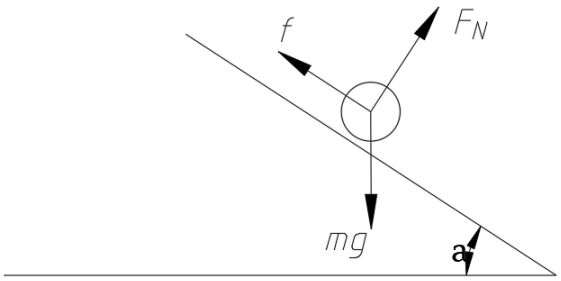

Figure 8. Force analysis diagram

When the screen surface is at the critical state of leaving the supporting surface, the normal force FN=0, it can be concluded that:

$$F_N = \frac{G}{g} \times A \times sinwt - G \times cosa = 0 \tag{3}$$

Introducing the formula for projection intensity:

$$K_v = \frac{1}{sin\varphi d} = \frac{A \times w^2}{g \times cos\, a} = \frac{K}{cos\, a} \tag{4}$$

φ_d—Adjust the Angle between the start and the slope
w—-Angular velocity

It can be concluded that when $K_v = 1$, the peanuts are at the critical state of sliding and bouncing on the screen surface. When $K_v > 1$, the peanuts bounce on the screen, and the greater the value, the more intense the bouncing. To simplify this process, let's assume α=0, The displacement x, velocity v_x, and acceleration of the peanuts within a given time are respectively a_x

$$x = -rcosat \tag{5}$$

$$v_x = ar\, sin\, at \tag{6}$$

$$a_x = \omega^2 r\, cos\, at \tag{7}$$

r - crank radius; a- Crank angular speed; t - Time.

As shown in Figure 1, through in-depth exploration of the behavior of peanuts on the screen surface, their motion patterns are subdivided into jumping and sliding. This analysis method further investigates the force conditions based on kinematics. When the maximum size of the raw material is smaller than the screen hole size, the peanuts will smoothly fall into the next layer, achieving grading and screening. With the help of multi-stage screening, peanuts can be effectively classified. After comprehensively considering the situation in Figure 1, it is found that peanuts are simultaneously affected by friction force f, supporting force FN, and air resistance pf during their movement. According

to the principles of kinematics, it can be derived that.

(1) Inertia force of peanut: $I = ma = ma^2 \cos at$;

(2) Friction force: $f = \mu F_n = tg\varphi F_n$

(3) Air resistance: $p_f = k\rho A v^2$

To achieve continuous screening of materials on the screen, the key lies in maintaining a directed motion path. This motion requires that the materials can only move in one direction. Assuming the materials are sliding forward, specific conditions must be set to ensure the realization of this reverse movement.

$$f = -p_f \cos\gamma + I\cos(\beta - a) - mg\sin a \tag{8}$$

Holding power:

$$F_N = -mg\cos a - I\sin(\beta - a) - p_f \sin\gamma \tag{9}$$

Take into account:

$$\left[mg\cos a - I\sin(\beta - a) - p_f \sin\gamma\right]tg\phi = -p_f \cos\gamma + I\cos(\beta - a) - mg\sin a \tag{10}$$

$$\begin{aligned} & mg(\cos a\sin\varphi + \sin a\cos\varphi) + p_f(\cos\gamma\cos\varphi - \sin\gamma\sin\varphi) \\ & = I\left[\cos(\beta - a)\cos\varphi + \sin(\beta - a)\sin\varphi\right]mg\sin(\varphi + a) + p_f\cos(\gamma + \varphi) \\ & = I\cos(\beta - a - \varphi)m\omega^2 r\cos\omega t \\ & = \frac{mg\sin(\varphi + a) + p_f\cos(\gamma + \varphi)}{\cos(\beta - a - \varphi)} \end{aligned} \tag{11}$$

Due to $\cos at \le 1$, the conditions for satisfying backslide are:

$$\frac{\omega^2 r}{g} \ge \frac{mg\sin(\varphi + a)p_f\cos(\gamma + \varphi)}{mg\cos(\beta - a - \varphi)} \tag{12}$$

To achieve uninterrupted screening of materials on the screen, their direction of motion must remain consistent, that is, moving linearly forward. To ensure this process, if the materials have a tendency to slide forward, then a necessary condition is to realize the reverse movement of the materials.

$$F = p_f\cos\gamma + mg\sin a + I\cos(\beta - a) \tag{13}$$

Holding power:

$$F_N = mg\cos a - I\sin(\beta - a) - p_f\sin\gamma \tag{14}$$

Bring in the data to obtain, meet the forward slip condition is:

$$\frac{\omega^{2r}}{g} \ge \frac{mg\sin(\varphi - a) - p_f(\gamma - \varphi)}{mg\cos(\beta - a - \varphi)} \tag{15}$$

If the I direction is to the right, its supporting force is:

$$F_N = mg\cos a - I\sin(\beta - a) - P_f\sin\gamma = mg\cos a - ma^2 r\cos a \times \sin(\beta - a)P_f\sin\gamma$$

keeping other conditions constant, once the angular acceleration rises to a certain point, the supporting force will drop to zero. This turning point marks the point where the angular velocity reaches the so-called "critical value for jumping." From this, a conclusion can be drawn:

$$\frac{\omega^2}{g} \ge \frac{mg\cos a - p_f\sin\gamma}{mg\sin(\beta - a)} \tag{16}$$

4.3. Vibrating screen structure size

Under the action of differential vibration, the raw materials are dumped into the vibrating screen, embarking on a unique journey. The peanuts cleverly slide through the hollow channels of the first-level screen, while the peanut kernels are guided to the next level of the screen to continue their fate of being screened. Each level of the screen is equipped with a unique outlet, making the separation process efficient and orderly.

Due to the extensive research, through consulting relevant materials, 15°is taken as the minimum interval to facilitate production, and 60° is chosen as the optimal vibration opening, with the opening rate accounting for 15%, and its structure is determined as shown in Figure9 below.

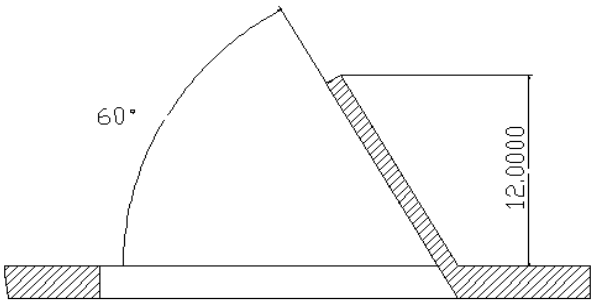

Figure 9. Vibration screen pass pattern

4.4. Fan selection

When selecting a ventilation device for peanut kernel selection, a specific volute centrifugal fan with a blade diameter precisely set at 200mm was chosen. The design of this fan allows its outlet to form an elegant 15-degree inclination with the horizontal plane. When deciding on the fan type, two core considerations are wind volume and wind pressure. Especially during the cleaning process of peanut kernels, the intensity of wind pressure plays a decisive role. There is a delicate balance between the number of blades and wind pressure: the more blades, the greater the wind pressure,

but this also means greater resistance. Therefore, it is necessary to find an ideal balance between these two factors. Through in-depth research of numerous literature and combining practical experience, the final selected fan model is SYP130/160, which achieves an ideal match between performance and efficiency, as shown in Figure 10.

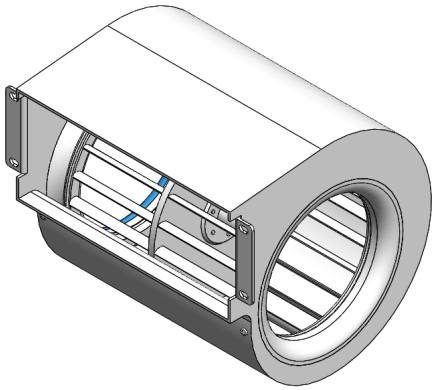

Figure 9. Fan structure diagram

5. Conclusion

(1) In the comprehensive design plan, an electric motor is employed as the core power system, and a hybrid cleaning strategy that combines vibration screening with air separation is innovatively proposed.

(2) The rubbing component in the peanut shelling machine is designed and its feasibility is verified through force analysis. In the design of the cleaning component, it is ultimately determined that the application of a curved vibrating screen in the peanut impurity removal system is more appropriate, aligning with the operational requirements for continuous and uninterrupted work of the peanut shelling machine.

References

[1] Bu Yunlong, Li Yingzhong, Long Zhiqiang et al. Research and development of light and simple belt conveying equipment for facility agriculture [J]. Agricultural Engineering Technology, 2019,41(31):23-27. (in Chinese)

[2] Kokieva G E,Badmaev Z V,Hamarova S V,Trofimova V S,Ivanova M N. High-Speed Efficient and Compact Screw Grain Conveyors in Agriculture[J]. IOP Conference Series: Earth and Environmental Science,2021,720(1).

[3] Ren Liang, Yu Shutao, Sun Hongxi et al. Analysis of agronomic characters and pod physical characteristics of peanut and screening of varieties suitable for mechanical husking [J/OL]. Molecular Plant Breeding, 1-12.

[4] Liu Z ,Yu Y ,Wang J , et al. Numerical Simulation and Optimization of Peanut Sheller Air–Screen Cleaning Device [J]. Agriculture, 2023, 13 (10):

[5] LIU S C. Optimization Design and Simulation Analysis of Key Components of low-damage peanut sheller [D]. Jilin Agricultural University, 2022.

[6] ZHANG Jinlong. Design and Simulation Analysis of Peanut sheller Parts with blade scraper [D]. Jilin Agricultural University, 2022.

[7] Jiannan W ,Huanxiong X ,Zhichao H , et al. Optimization of Material for Key Components and Parameters of Peanut Sheller Based on Hertz Theory and Box–Behnken Design [J]. Agriculture, 2022, 12 (2): 146-146.

[8] ZHANG Yuandong, Wang Dongwei, He Xiaoning et al. Simulation research on husking force of peanut pod based on Workbench LS-dyna [J]. Journal of Peanut Science, 2022, 51 (01): 66-71.

[9] LU R. Research on the Principle and key technology of Peanut sheller with vertical cone drum [D]. Shenyang Agricultural University, 2020.

[10] Fannou C L J ,Semassou C G ,Chegnimonhan V K , et al. Design and Manufacture of a Groundnut Sheller [J]. Journal of Experimental Agriculture International, 2020, 66-75.